Journal of Computers Vol. 35 No. 2, April 2024, pp. 37-57
doi: 10.53106/199115992024043502003

Robust Energy Efficiency Optimization Strategy for Emergency Communication Based on Fixed-Wing UAV

Jia-Rong Cao[1,2], Wei Wang[1,2,3*], Na Xu[1,2], Wen-Ting Su[1,2],
Long-Xing Xing[1,2], Jia-Tao Su[1,2]

[1] School of Information and Electrical Engineering, Hebei University of Engineering,
Handan, 056038, Hebei, China
[2] Hebei Key Laboratory of Security and Protection Information Sensing and Processing,
Handan, 056038, Hebei, China
{caojiarong130, gengu139}@163.com, {1979787361, 1552311309, 438558705}@qq.com
[3] School of Internet of Things Engineering, Jiangnan University,
Wuxi, 214122, Jiangsu, China
wangwei83@hebeu.edu.cn

Received 25 July 2023; Revised 5 December 2023; Accepted 3 January 2024

Abstract. The geographic location information of a user serves as the foundation for post-disaster emergency applications. However, uncertainties in the user positioning may arise due to factors such as building obstruction and damage to ground base stations. To ensure optimal communication quality, unmanned aerial vehicles (UAVs) can be implemented to maintain close proximity to the user with a minimal turning radius. However, a small turning radius can result in increased energy consumption due to propulsion requirements. To achieve an optimal balance between high communication throughput and low energy consumption, a robust energy efficiency optimization strategy is proposed based on a fixed-wing UAV, addressing the energy efficiency of emergency communication in imprecise user locations. First, the air-to-ground channel model is established, taking into account UAV propulsion energy consumption and formulating a multi-constraint problem to maximize emergency energy efficiency. Second, by incorporating the circular region method to address location uncertainty and considering the worst-case scenario, a robust problem is formulated. Finally, the worst-case scenario is addressed by utilizing the first-order Taylor approximation and successive convex approximation (SCA) technique to solve the nonconvex problem. Through simulation experiments, the proposed scheme is compared with three benchmark schemes, demonstrating its superior energy efficiency and robustness.

Keywords: UAV emergency communications, energy efficiency optimization, robustness

1 Introduction

Post-disaster emergency scenarios are characterized by suddenness, environmental complexity and communication urgency. When infrastructure is damaged in a disaster event, it becomes difficult to restore ground communications quickly within a short period of time, which poses a major obstacle to providing emergency communication support at disaster-relief sites. Fortunately, with the rapid development of science and technology, disaster emergency rescue events can be responded to more quickly, safely, and effectively by constructing an integrated sky and ground network architecture and deploying communication nodes under extreme conditions such as disconnection, power outage, and network interruption [1]. As a new type of emergency communication equipment, UAVs have many advantages, such as on-demand deployment, high mobility, and line-of-sight (LoS) links [2]. Although these advantages of UAV-assisted emergency communication make high-speed transmission between air and ground possible, they also bring intractable challenges that cannot be ignored, among which the limited onboard energy of UAVs is a key practical issue [3].

In disaster emergency events, location information is crucial for key applications such as wireless information transmission, the effective allocation of emergency resources, and emergency resource scheduling [4]. However, various factors, such as inaccurate positioning accuracy of the equipment, building occlusion, and environmental interference, prevent heterogeneous devices from obtaining precise location information of the user, which

* Corresponding Author

impacts rescue efficiency [5]. In this case, studying the robust optimization strategy of UAV emergency communication energy efficiency is imperative to meet the communication requirements in resource-constrained post-disaster rescue environments. The focus of previous studies was primarily on optimizing the throughput [6] and energy consumption [7] of UAV communication based on the deterministic model. However, at present, there is a lack of comprehensive research on the joint optimization problem of UAV energy consumption and communication throughput affected by location information uncertainty.

To ensure the reliability of communication links, reduce energy consumption and improve energy efficiency, a robust energy-saving optimization strategy is proposed in this paper for emergency communication based on fixed-wing UAVs, considering the uncertainty of user location information in disaster emergency rescue and balancing the flight energy consumption and communication rate of UAVs. The optimization scheme proposed in this paper further advances the existing research in the field of UAV-assisted emergency communication and extends the deterministic model of UAV emergency communication, which has important theoretical significance and practical value.

The rest of the paper is structured as follows: In Section 2, related works on UAVs that are used as airborne base stations or relays are presented. The air-ground channel model and the UAV propulsion energy consumption model are presented in Section 3. In Section 4, the problem of robust energy efficiency optimization is described, and the solution procedure, along with the algorithm design scheme, is presented. The simulation parameters are provided in Section 5, where the simulation experiments are conducted, the proposed scheme is compared with other schemes, and the numerical results are presented. Finally, in Section 6, this work is concluded with some suggestions for future work.

2 Related Work

Recently, UAVs have primarily been utilized as airborne base stations or relays for signal coverage, relay forwarding, and broadcast communication. Among these applications, information throughput serves as a crucial metric for assessing the quality of communication. In [8], the UAV transmitted information to multiple ground nodes, and the joint optimization of UAV trajectory and power was alternately executed to maximize the information throughput. In [9], the UAV acted as an aerial relay to optimize end-to-end throughput by jointly optimizing its trajectory, transmission power, and information source. The authors in [10] investigated the joint optimization of UAV trajectory and power allocation to maximize the minimum achievable average communication rate for users. The authors in [11] proposed a reinforcement learning-based joint optimization algorithm for multi-UAV trajectory and transmission power, aiming to maximize the instantaneous total transmission rate by accurately predicting user mobility information. The authors in [12] explored the issue of secure communication with UAVs acting as base stations, assisted by intelligent reflecting surfaces, the objective is to maximize the rate of secure transmission while minimizing complexity.

However, the above work focused solely on optimizing throughput in UAV communication and disregarded energy consumption, which is a concern due to limited onboard energy. Therefore, scholars are increasingly interested in developing efficient and energy-saving communication methods. In [13], the trajectory of the UAV was optimized to minimize energy consumption. In [14], the optimization of UAV energy consumption was achieved through joint optimization of trajectory, task offloading, and CPU control. The authors in [15] investigated the minimization of maximum energy consumption for all ground devices, while ensuring data reception and required 3D positioning performance.

The above work only considers the problem of optimizing throughput or minimizing energy consumption. On the one hand, to ensure that the ground user receives information faster or more information, the UAV needs to be as close to the user as possible. For rotary-wing UAVs, this means increasing propulsion energy consumption to maintain hovering operations, while fixed-wing UAVs are less likely to perform strict zero-velocity hovering [16]. On the other hand, sacrificing the propulsion energy consumption is not an optimal choice for enabling the ground user to obtain more information transmission. Therefore, there is a trade-off between UAV propulsion energy consumption and communication throughput. To achieve optimal balance between the two, researchers have introduced the concept of energy efficiency as a measure of energy-efficient communication. In [16], a fixed-wing UAV energy consumption model was developed to optimize the trajectory, speed, and acceleration of the UAV at a constant altitude in order to maximize its energy efficiency. In [17], joint optimization of trajectory, velocity, and acceleration was employed to maximize the energy efficiency of the UAV. The authors in [18] proposed an efficient iterative algorithm based on block coordinate descent (BCD) and SCA techniques to jointly optimize the transmit power of the ground source node and the UAV, as well as the flight trajectory of the UAV, aiming to maximize the safety and energy efficiency of the UAV system.

All the aforementioned studies have modeled the communication network of UAVs as either an air base station or a relay node, utilizing deterministic models. Their objective is to optimize energy efficiency in UAV communication by regulating power and optimizing trajectory. In the UAV-assisted emergency communication model, precise positioning information of ground users is essential for relevant research. However, factors such as the positioning devices, algorithms, and environmental interference can impact the accuracy of coordinate data during emergency situations. Given the uncertainty of information, researchers have been focusing on ensuring that existing algorithms are robust enough to mitigate or eliminate its impact. Currently, research in this area primarily focuses on achieving secure and resilient transmission for UAVs [19-21], as well as enhancing aircraft attitude control with greater resilience [22-23]. Table 1 presents the optimization objectives, technologies, advantages, and limitations of the related work that rely on deterministic models for research.

In summary, most scholars in the field of UAV-assisted communication heavily rely on establishing deterministic optimization models for their research. However, during disaster emergency response, the user location information may contain errors due to building obstructions, environmental interference and other factors. Therefore, relying solely on deterministic models for research methods is no longer feasible. The user's location in the UAV-assisted emergency communication system affects the quality of communication, thereby directly impacting the overall system performance. In disaster emergency scenarios, to ensure that the UAV can meet the communication rate requirements while consuming low energy, this paper considers the introduction of uncertainty into the model and focuses on optimizing the energy efficiency problem of air-to-ground communication, taking into account the uncertainty of user location information.

The main contributions of the paper are summarized as follows:

(1) In this paper, an energy efficiency model for emergency communication based on the fixed-wing UAV is established. The air-ground channel model and the theoretical model on the propulsion energy consumption of fixed-wing UAVs dependence on speed and acceleration are developed. A multi-constrained problem is formulated with the objective of maximizing energy efficiency.

(2) The circular region method is employed to characterize the uncertainty of user location information, and a robust energy efficiency optimization problem is formulated. By considering the worst-case scenario, the optimization model with the uncertain parameter is transformed into a deterministic form. Subsequently, an optimization problem for robust energy efficiency is established based on the coordinate error, and its algorithmic steps are presented.

(3) The simulation results demonstrate that the proposed scheme can mitigate the impact of uncertainty, enhancing energy efficiency, and improving robustness. The effectiveness of this approach is validated by comparing it with three benchmark schemes and analyzing the impact of errors on system performance.

Table 1. The related work that relies on deterministic models

Reference number	Optimization objective	Technology	Advantage	Limitation
[8]	Throughput	SCA	Multiple ground nodes	The problem of limited onboard energy of UAV is not considered
[9]	End-to-end throughputs	SCA	Multiple UAV relays	
[10]	The minimum achievable average rate among users	Penalty dual-decomposition	Non-orthogonal multiple access	
[11]	The instantaneous sum transmit rate	Multi-agent Q-learning	The prediction of users' mobility information	
[12]	The average secrecy rate	SCA	Intelligent reflecting surface	
[13]	The total UAV energy consumption	SCA	Multiple ground nodes	The issue of throughput is not considered
[14]	The total required energy	SCA	Piecewise nonlinear energy harvesting model	
[15]	The maximum energy consumption of all devices	Differential evolution	Device positioning	
[16]	Energy efficiency	SCA	The propulsion energy consumption	The uncertainty factor in the model is not considered
[17]	Energy efficiency	SCA	Multiple ground nodes	
[18]	The maximum energy efficiency	BCD, SCA	The residual self-interference	

3 System Model

In the event of damage to the ground base station caused by external factors such as natural disasters, it is assumed that a single antenna-equipped fixed-wing UAV flying in the air can restore communication and provide downlink wireless transmission services for ground users in emergency areas.

As shown in Fig. 1, a fixed-wing UAV emergency communication system model is considered. It is assumed that there is a sole ground user and a fixed-wing UAV equipped with a single antenna operating within the airspace of an emergency area. The position of the ground user remains stationary, while the ground base station has incurred damage due to external factors such as natural disasters. The UAV is responsible for reestablishing communication and delivering wireless transmission services to the ground user within the designated area.

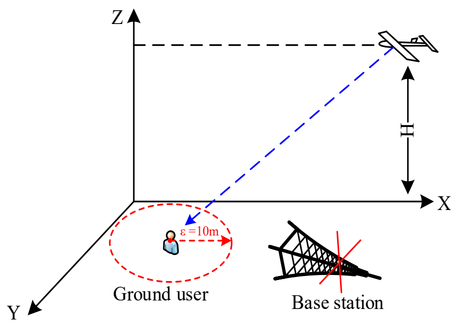

Fig. 1. Emergency communication from a fixed-wing UAV to a ground user

3.1 Channel Model

Without loss of generality, a three-dimensional (3D) Cartesian coordinate system is considered. In practical applications, the limited onboard energy of the UAV necessitates careful management of propulsion resources due to significant consumption during frequent ascents or descents. To reduce the energy consumption of the UAV and ensure sufficient flight time, it is assumed that the UAV will flies at a constant altitude H, which should be maintained at a low enough level to avoid frequent ascents and descents, as well as any obstacles such as terrain or buildings.

To enhance the precision of UAV positioning, the discrete approximation method is employed to model its flight trajectory. The continuous flight time T is divided into $N+2$ equal-length quasi-static time slots with step size δ_t , i.e., $t = n\delta_t$, $n = 0, 1, ..., N + 1$. Assuming that the step size δ_t is sufficiently small, it can be approximated that the distance between the UAV and the ground user remains constant within each time slot. Therefore, the projected flight trajectory of the UAV on the horizontal plane can be approximated as $\mathbf{q}[n] = [x_n, y_n]^T$, $n \in \{0,1,\dots,N+1\}$. The precise location of the ground user is indicated by $\mathbf{p}$. Thus, the actual distance between the UAV and the ground user can be represented as:

$$d[n]=\sqrt{H^2+\|\mathbf{q}[n]-\mathbf{p}\|_2^2}\ , \tag{1}$$

where, $\|\cdot\|_2$ represents the 2-norm. Due to the high altitude and LoS link characteristics inherent in UAV, it is assumed that the primary mode of communication between the UAV and the ground user is through the LoS channel. Furthermore, it is presumed that any potential Doppler shift in communication can be effectively compensated for by the receiver located at the ground user's end. The power gain $h[n]$ between the UAV and the ground user in the wireless channel at time slot n is determined by the free-space path loss model, which can be mathematically expressed as:

$$h[n] = \beta_0 d^{-2}[n] = \frac{\beta_0}{H^2 + \| \mathbf{q}[n] - \mathbf{p} \|_2^2} \ , \tag{2}$$

where β_0 denotes the wireless channel power gain at reference distance d_0 = 1m. Assuming a constant maximum transmission power p for the UAV, the communication link capacity $R[n]$ at time slot n can be expressed as:

$$R[n] = B\delta_t \log_2\left(1 + \frac{\gamma_0}{H^2 + \| \mathbf{q}[n] - \mathbf{p} \|_2^2}\right) \ , \tag{3}$$

where B represents the channel bandwidth, $\gamma_0 = \frac{p\beta_0}{\sigma^2}$ denotes the reference received signal-to-noise ratio (SNR) under condition $d_0 = 1m$, where σ^2 stands for the power of additive white Gaussian noise at the receiver of the ground user. In case additional interference is present at the receiver, it is assumed to follow a Gaussian distribution and its power can be incorporated within term σ^2 as part of the overall noise.

3.2 Fixed-Wing UAV Propulsion Energy Consumption Model

Fixed-wing UAVs typically possess larger payloads and higher speeds compared to rotary-wing UAVs. The overall energy consumption associated with their communication with the ground user generally consists of two components: one pertains to the energy consumed during communication, while the other relates to the propulsion energy required for maintaining high altitude and facilitating mobility. In practical applications, the energy consumption for propulsion of fixed-wing UAVs is significantly higher than that for communication. This paper solely focuses on the energy consumption necessary to maintain high-altitude flight, denoted as $E[n]$. The model representing the energy consumption of the fixed-wing UAV at time slot n, as a function of flight speed, direction, and acceleration, is expressed as:

$$E[n] = \delta_t\left[u_1\|\mathbf{v}[n]\|_2^3 + \frac{u_2}{\|\mathbf{v}[n]\|_2}\left(1 + \frac{\|\mathbf{a}[n]\|_2^2}{g_a^2}\right)\right] + \Delta_k \ , \tag{4}$$

where μ_1 and μ_2 are two constant parameters related to gravity, encompassing the fuselage and all loads, wing area, air density, etc., $g_a = 9.8m / s^2$ denotes the acceleration of gravity, and Δ_k represents the change in kinetic energy of the UAV, which is calculated as:

$$\Delta_k = \frac{1}{2} m\left(\| v[N+1] \|_2^2 - \| v[0] \|_2^2\right) \ , \tag{5}$$

where $v[0]$ and $v[N + 1]$ represent the initial and final velocities of the UAV respectively, while m represents its mass. $\mathbf{v}[n]$ denotes the velocity of the UAV, which corresponds to the first derivative of the UAV trajectory $\mathbf{q}[n]$. On the other hand, $\mathbf{a}[n]$ denotes the acceleration of the UAV, which corresponds to the second derivative of $\mathbf{q}[n]$. $\mathbf{v}[n]$ and $\mathbf{a}[n]$ can be expressed as:

$$\mathbf{v}[n] \triangleq \dot{\mathbf{q}}[n] \ , \tag{6}$$

$$\mathbf{a}[n] \triangleq \ddot{\mathbf{q}}[n] \ . \tag{7}$$

Therefore, $\mathbf{a}[n] \triangleq \dot{\mathbf{v}}[n]$,the acceleration $\mathbf{a}[n]$ is the first derivative of the velocity $\mathbf{v}[n]$. Thus, for any infinitesimal time step δ_t , we have following results based on the first- and second-order Taylor approximations,

$$\mathbf{v}[n+1]=\mathbf{v}[n]+\mathbf{a}[n]\delta_t,\ n=0,\ldots,N\ , \tag{8}$$

$$\mathbf{q}[n+1]=\mathbf{q}[n]+\mathbf{v}[n]\delta_t+\frac{1}{2}\mathbf{a}[n]\delta_t^2,\ n=0,\ldots,N\ . \tag{9}$$

4 Problem Description and Solution

In order to ensure that the UAV meets the energy-efficient communication requirements with the ground users without excessive consumption of onboard energy, a deterministic optimization model [16] is established with the goal of maximizing the energy efficiency. Energy efficiency, defined as the ratio of communication throughput to propulsion energy consumption. Considering the suddenness and uncertainty of disaster emergency events, traditional deterministic system models tend to ignore the influence of uncertainty conditions on the model. In order to solve this problem, this paper describes the uncertainty in location information and introduces a specific deterministic optimization model, and reconstructs the air-ground communication energy efficiency optimization model with uncertainty, so as to achieve the purpose of efficient and stable communication.

4.1 Communication Energy Efficiency Optimization Problem

According to the established channel and energy consumption models for the fixed-wing UAV, the actual performance constraints of UAV in emergency rescue situations are further taken into consideration. The energy-efficiency maximization problem in emergency communication based on the fixed-wing UAV can be formulated as:

$$(\text{P1}):\ \max_{\{\mathbf{q}[n],\mathbf{v}[n],\mathbf{a}[n]\}} \frac{\mathrm{B}\sum_{n=1}^{N}\log_2\left(1+\frac{\gamma_0}{H^2+\|\mathbf{q}[n]-\mathbf{p}\|_2^2}\right)}{\sum_{n=1}^{N}\left[u_1\|\mathbf{v}[n]\|_2^3+\frac{u_2}{\|\mathbf{v}[n]\|_2}\left(1+\frac{\|\mathbf{a}[n]\|_2^2}{g_{\mathrm{a}}^2}\right)\right]+\frac{\Delta_k}{\delta_t}}\ , \tag{10a}$$

$$\text{s.t.}\quad \mathrm{C}_1:\mathbf{q}[0]=\mathbf{q}_0\ , \tag{10b}$$

$$\mathrm{C}_2:\mathbf{q}[N+1]=\mathbf{q}_F\ , \tag{10c}$$

$$\mathrm{C}_3:\mathbf{v}[0]=\mathbf{v}_0\ , \tag{10d}$$

$$\mathrm{C}_4:\mathbf{v}[N+1]=\mathbf{v}_F\ , \tag{10e}$$

$$\mathrm{C}_5:\mathbf{v}[n+1]=\mathbf{v}[n]+\mathbf{a}[n]\delta_t,n=0,\ldots,N\ , \tag{10f}$$

$$\mathrm{C}_6:\mathbf{q}[n+1]=\mathbf{q}[n]+\mathbf{v}[n]\delta_t+\frac{1}{2}\mathbf{a}[n]\delta_t^2,n=0,\ldots,N\ , \tag{10g}$$

$$\mathrm{C}_7:\|\mathbf{v}[n]\|_2\le V_{max},n=1,\ldots,N\ , \tag{10h}$$

$$\mathrm{C}_8:\|\mathbf{v}[n]\|_2\ge V_{min},n=1,\ldots,N\ , \tag{10i}$$

$$\mathrm{C}_9:\|\mathbf{a}[n]\|_2\le a_{max},n=1,\ldots,N\ , \tag{10j}$$

where C_1, C_2 denote the constraints on UAV takeoff and landing positions, $\mathbf{q}_0,\mathbf{q}_F\in\mathbb{R}^{2\times1}$ represent the initial and final positions, respectively, C_3, C_4 are the initial and final velocity constraints, $\mathbf{v}_0,\mathbf{v}_F\in\mathbb{R}^{2\times1}$ are the initial and final velocities. since $\mathbf{v}[n]\triangleq\dot{\mathbf{q}}[n]$, $\mathbf{a}[n]\triangleq\dot{\mathbf{v}}[n]$, C_5, C_6 can be derived from expression (8) and expression (9). C_7, C_8 represent the upper and lower limits of the UAV's flight speed, where V_{max} , V_{min} represent the maximum and minimum speed. Additionally, C_9 corresponds to the constraint on maximum acceleration, with a_{max} denotes the maximum acceleration.

4.2 Robust Energy Efficiency Optimization Problem

Description of Ground User Position Coordinate Error. In emergency situations such as disaster rescue, it is difficult to obtain accurate user location information due to factors such as poor network quality, positioning algorithm errors, environmental interference and asynchronous updates of coordinate information data. The robustness and energy efficiency of the system can be significantly reduced by this. To address this issue, an error model for the ground user position coordinate is established based on the circular region modeling method [24].

Assuming that the actual horizontal coordinate of the ground user $\mathbf{p} = [x_{GU}, y_{GU}]^T$ is unknown, while the estimated horizontal coordinate $\tilde{\mathbf{p}} = [\tilde{x}_{GU}, \tilde{y}_{GU}]^T$ is known. The relationship between $\mathbf{p}$ and $\tilde{\mathbf{p}}$ can be expressed as:

$$\mathbf{p} = \tilde{\mathbf{p}} + \mathbf{\Delta p} \ , \tag{11}$$

where $\mathbf{\Delta p} = [\Delta x_{GU}, \Delta y_{GU}]^T$ represents the estimation error, denoting the uncertainty of actual position coordinates of the ground user, while Δx_{GU}, Δy_{GU} represent the estimation error of x_{GU} , y_{GU} respectively, subject to the following constraints,

$$\Delta x_{GU}^2 + \Delta y_{GU}^2 \le \varepsilon^2 \ , \tag{12}$$

where ε denotes the acceptable margin of error, Thus, the following result is obtained,

$$\mathbf{\Delta p} \in \Phi \triangleq \left\{ \mathbf{\Delta p} \middle| \ \| \mathbf{p} - \tilde{\mathbf{p}} \|_2^2 \le \varepsilon^2 \right\} \ , \tag{13}$$

where Φ represents the set of position coordinate errors for the ground user located within a circular area centered at $(x_{GU}, y_{GU}, 0)$ with a radius of ε.

Uncertainty Transformation. In order to mitigate the impact of position uncertainty caused by incomplete knowledge of the actual ground user coordinates in (P1), expression (11) relating exact and estimated positions in the ground user position coordinate error model is first substituted into distance expression (1), which can be expressed as:

$$d[n] = \sqrt{H^2 + \| \mathbf{q}[n] - \mathbf{p} \|_2^2} = \sqrt{H^2 + \| \mathbf{q}[n] - (\tilde{\mathbf{p}} + \mathbf{\Delta p}) \|_2^2} = \sqrt{H^2 + \| \mathbf{q}[n] - \tilde{\mathbf{p}} - \mathbf{\Delta p} \|_2^2} \ . \tag{14}$$

Second, taking into account the worst-case scenario of wireless transmission where the ground user is located at a relatively far distance from the fixed-wing UAV and combining it with error expression (13), Additionally, the upper bound of the actual transmission distance $d[n]$ can be expressed as:

$$d[n] \le \sqrt{H^2 + | \| \mathbf{q}[n] - \tilde{\mathbf{p}} \|_2 + \| \mathbf{\Delta p} \|_2 |^2} \le \sqrt{H^2 + | \| \mathbf{q}[n] - \tilde{\mathbf{p}} \|_2 + \varepsilon |^2} \ . \tag{15}$$

Incorporating the distance upper bound expression (15) into the information throughput expression (3), the lower bound [25] of $R[n]$ at slot n can be expressed as:

$$R[n] \ge R_{lb}[n] = B\delta_t \log_2 \left(1 + \frac{\gamma_0}{H^2 + | \| \mathbf{q}[n] - \tilde{\mathbf{p}} \|_2 + \varepsilon |^2} \right) \ . \tag{16}$$

By substituting the information throughput lower bound expression (16) into (P1), the problem of maximizing robust energy efficiency in the worst case (P2) can be formulated as:

$$(\text{P2}):\max_{\{\mathbf{q}[n],\mathbf{v}[n],\mathbf{a}[n]\}} \frac{\mathrm{B}\sum_{n=1}^{N}\log_2\left(1+\dfrac{\gamma_0}{H^2+|\|\mathbf{q}[n]-\tilde{\mathbf{p}}\|_2+\varepsilon|^2}\right)}{\sum_{n=1}^{N}\left[u_1\|\mathbf{v}[n]\|_2^3+\dfrac{u_2}{\|\mathbf{v}[n]\|_2}\left(1+\dfrac{\|\mathbf{a}[n]\|_2^2}{g_{\mathrm{a}}^2}\right)\right]+\dfrac{\Delta_k}{\delta_t}}, \quad \textbf{(17a)}$$

$$\text{s.t.} \qquad \mathrm{C}_1-\mathrm{C}_9 . \quad \textbf{(17b)}$$

(P2) is a typical fractional programming problem [26], where the numerator of the objective function is non-concave and the denominator is nonconvex. As such, (P2) cannot be considered a convex problem and it poses difficulties for direct solution using standard convex optimization techniques. The SCA technique is adopted to address this issue more effectively.

Transformation of Convex Optimization Problem. As the constraints $\mathrm{C}_1-\mathrm{C}_7$ and C_9 in (P2) are convex, while the minimum velocity constraint C_8 is nonconvex, it is necessary to convert C_8 into a convex constraint for solving (P2). By introducing the relaxation variable $\{\upsilon_n\}$, (P2) can be reformulated as:

$$(\text{P3}):\max_{\substack{\{\mathbf{q}[n],\mathbf{v}[n],\\ \mathbf{a}[n],\upsilon_n\}}} \frac{B\sum_{n=1}^{N}\log_2\left(1+\dfrac{\gamma_0}{H^2+|\|\mathbf{q}[n]-\tilde{\mathbf{p}}\|_2+\varepsilon|^2}\right)}{\sum_{n=1}^{N}\left[u_1\|\mathbf{v}[n]\|_2^3+\dfrac{u_2}{\upsilon_n}+\dfrac{u_2\|\mathbf{a}[n]\|_2^2}{g_{\mathrm{a}}^2\upsilon_n}\right]+\dfrac{\Delta_k}{\delta_t}}, \quad \textbf{(18a)}$$

$$\text{s.t.} \qquad \mathrm{C}_1-\mathrm{C}_7,\mathrm{C}_9 , \quad \textbf{(18b)}$$

$$\mathrm{C}_{10}:\upsilon_n\ge V_{min},\forall n , \quad \textbf{(18c)}$$

$$\mathrm{C}_{11}:\|\mathbf{v}[n]\|_2^2\ge\upsilon_n^2,\forall n . \quad \textbf{(18d)}$$

At the optimal solution of (P3), there must have $\upsilon_n=\|\mathbf{v}[n]\|_2,\forall n$, otherwise, increasing υ_n would result in a strictly higher objective value, thus (P3) is equivalent to (P2). At this juncture, the denominator of the objective function in (P3) is convex with respect to $\{\mathbf{v}[n], \mathbf{a}[n], \upsilon_n\}$, however a new nonconvex constraint C_{11} has emerged. To simplify the problem-solving process, the first-order Taylor approximation [27] is applied to relax constraint C_{11} for any local point $\{\mathbf{v}_j[n]\}$ obtained in the jth iteration, which can be expressed as:

$$\|\mathbf{v}[n]\|_2^2\ge\|\mathbf{v}_j[n]\|_2^2+2\mathbf{v}_j^T[n](\mathbf{v}[n]-\mathbf{v}_j[n])=\Psi_{lb}(\mathbf{v}[n]),\forall\mathbf{v}[n] , \quad \textbf{(19)}$$

where the equality holds at $\mathbf{v}[n]=\mathbf{v}_j[n]$. Define the new constraint C_{12} as follows:

$$\mathrm{C}_{12}:\Psi_{lb}(\mathbf{v}[n])\ge\upsilon_n^2,\forall n . \quad \textbf{(20)}$$

The convexity of constraint C_{12} is attributed to the linearity of $\Psi_{lb}(\mathbf{v}[n])$ in relation to $\mathbf{v}[n]$.

Subsequently, the molecular constituent of the optimization function in (P3) is taken into account. To convert it into a convex function form, we also employ first-order Taylor approximation to relax any local point $\{\mathbf{q}_j[n]\}$ obtained by jth iteration and define the function $\overline{R}_{lb}(\{\mathbf{q}[n]\})$ as follows:

$$\overline{R}_{lb}(\{\mathbf{q}[n]\})=B\delta_t\sum_{n=1}^{N}\Big[\alpha_j[n]-\beta_j[n]\big(|\|\mathbf{q}[n]-\tilde{\mathbf{p}}\|_2+\varepsilon|^2-|\|\mathbf{q}_j[n]-\tilde{\mathbf{p}}\|_2+\varepsilon|^2\big)\Big] , \quad \textbf{(21)}$$

where:

$$\alpha_j[n] = \log_2\left(1+\frac{\gamma_0}{H^2+|\|\mathbf{q}_j[n]-\tilde{\mathbf{p}}\|_2+\varepsilon|^2}\right), \tag{22}$$

$$\beta_j[n] = \frac{\left(\log_2^{\,e}\right)\gamma_0}{\left(H^2+\gamma_0+|\|\mathbf{q}_j[n]-\tilde{\mathbf{p}}\|_2+\varepsilon|^2\right)\left(H^2+|\|\mathbf{q}_j[n]-\tilde{\mathbf{p}}\|_2+\varepsilon|^2\right)}. \tag{23}$$

Note that $\overline{R}_{lb}(\{\mathbf{q}[n]\})$ is a concave function with respect to $\{\mathbf{q}[n]\}$, for any given $\{\mathbf{q}_j[n]\}$ there are the following result,

$$R_{lb}[n] = B\delta_t \log_2\left(1+\frac{\gamma_0}{H^2+|\|\mathbf{q}[n]-\tilde{\mathbf{p}}\|_2+\varepsilon|^2}\right) \geq \overline{R}_{lb}(\{\mathbf{q}[n]\}), \forall \mathbf{q}[n], \tag{24}$$

where the equality holds at $\mathbf{q}[n]=\mathbf{q}_j[n], \forall n$, whereby the ultimate solution for any given local point $\{\mathbf{q}_j[n], \mathbf{v}_j[n]\}$ can be represented as:

$$(\text{P4}): \max_{\substack{\{\mathbf{q}[n],\mathbf{v}[n],\\ \mathbf{a}[n],\upsilon_n\}}} \frac{B\sum_{n=1}^{N}\left[\alpha_j[n]-\beta_j[n]\left(|\|\mathbf{q}[n]-\tilde{\mathbf{p}}\|_2+\varepsilon|^2-|\|\mathbf{q}_j[n]-\tilde{\mathbf{p}}\|_2+\varepsilon|^2\right)\right]}{\sum_{n=1}^{N}\left[u_1\|\mathbf{v}[n]\|_2^3+\frac{u_2}{\upsilon_n}+\frac{u_2\|\mathbf{a}[n]\|_2^2}{g_a^2\upsilon_n}\right]+\frac{\Delta_k}{\delta_t}}, \tag{25a}$$

$$\text{s.t.} \quad C_1 - C_7, C_9, \tag{25b}$$

$$C_{10}: \upsilon_n \geq V_{min}, \forall n, \tag{25c}$$

$$C_{12}: \Psi_{lb}(\mathbf{v}[n]) \geq \upsilon_n^2, \forall n. \tag{25d}$$

As the numerator of (P4)'s objective function is concave, the denominator is convex, and the constraints are also convex, (P4) can be classified as a convex optimization problem that can be solved using standard tools such as CVX [28]. Algorithm 1 outlines the process of solving based on SCA technology.

4.3 Algorithm Design

Comprehensive analysis, Algorithm 1 provides the pseudocode of the robust energy efficiency optimization algorithm based on SCA, as shown in Table 2.

Table 2. The pseudo code of the Algorithm 1

Algorithm 1. Robust energy efficiency optimization algorithm based on SCA
1: Initialize $\mathbf{q}_0[n], \mathbf{v}_0[n], \forall n,$ let $j=0$
2: Repeat
3: Solve (P4) for the given local point $\{\mathbf{q}_j[n], \mathbf{v}_j[n]\}$, and denote the optimal solution as $\{\mathbf{q}_j^*[n], \mathbf{v}_j^*[n]\}$
4: Update the local point $\mathbf{q}_{j+1}[n]=\mathbf{q}_j^*[n]$ and $\mathbf{v}_{j+1}[n]=\mathbf{v}_j^*[n]$, $\forall n$
5: Update $j=j+1$
6: Until the fractional increase of the objective value of (P3) is below a threshold 0.1%

5 Simulation and Analysis

5.1 Simulation Parameters

In this section, the proposed design is validated through numerical results. In this paper, the simulation experiment is carried out using the simulation software of Matlab. Let $\mathbf{q}_0 = [0, 1000]^T$, $\mathbf{q}_F = [1000, 0]^T$, $\mathbf{v}_0 = \mathbf{v}_F = 30\vec{\mathbf{v}}_{0F}$, with $\vec{\mathbf{v}}_{0F} \triangleq (\mathbf{q}_F - \mathbf{q}_0)/\|\mathbf{q}_F - \mathbf{q}_0\|$ denoting the direction from $\mathbf{q}_0$ to $\mathbf{q}_F$, $\mathbf{p} = [0, 0]^T$ denotes the precise position of the ground user. In Algorithm 1, the initial points are set to be the straight flight from $\mathbf{q}_0$ to $\mathbf{q}_F$ with constant velocity. Other simulation parameters are shown in Table 3.

5.2 Analysis of Simulation Results

The convergence curves of the proposed scheme and the optimization scheme, which is based on the deterministic model proposed in [16], are shown in Fig. 2. In the figure, EE-max represents the convergence curve of the scheme proposed in [16], RobustEE-max represents the convergence curve of the optimization scheme proposed in this paper, and the termination threshold of Algorithm 1 is 0.1%. In the EE-max scheme, the location information of the ground user is known and fixed at [0, 0]. However, the RobustEE-max scheme takes into account the interference in the emergency rescue environment, which leads to inaccurate acquisition of location information. Therefore, the proposed scheme sets the estimated coordinates of the ground user to [50,50], i.e., $\tilde{\mathbf{p}} = [50, 50]^T$, and the estimation error to 10, i.e., $\varepsilon = 10$. The UAV flight time is $T = 260s$.

As shown in Fig. 2, in terms of convergence speed, the robust energy efficiency value of the RobustEE-max scheme at the 7th iteration exceeds 99.2% of the energy efficiency value of the EE-max scheme. From the perspective of convergence accuracy, the robust energy efficiency value of the RobustEE-max scheme remains within a deviation of 0.3% deviation from the energy efficiency value of the EE-max scheme. This is because the proposed scheme is designed for emergency rescue scenarios, where the acquisition of location information is uncertain due to environmental interference and other factors. The deterministic model-based optimization scheme is no longer applicable in such cases. The proposed scheme optimizes for worst-case scenarios while achieving similar convergence effects as that based on a deterministic model, indicating its ability to achieve convergence in 7 iterations considering the uncertainty of the user location. Therefore, the proposed scheme is verified to be effective and convergent.

Table 3. Simulation parameter

Parameter	Description	Value
H	Altitude	100m
B	Communication bandwidth	1MHz
N_0	Noise power spectral density	-170dBm/Hz
σ^2	Additive gaussian white noise power	-110dBm
β_0	Reference channel power gain	-50dB
P	Transmitting power	10dBm/0.01W
γ_0	Signal-to-noise ratio	30dB
u_1	Constant parameter 1	9.24×10^{-4}
u_2	Constant parameter 2	2250
V_{max}	Maximum UAV speed	100m/s
V_{min}	Minimum UAV speed	3m/s
a_{max}	Maximum UAV acceleration	5m/s^2
δ_t	Time slot length	0.2s

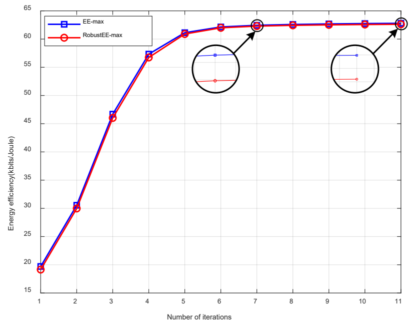

Fig. 2. Convergence verification

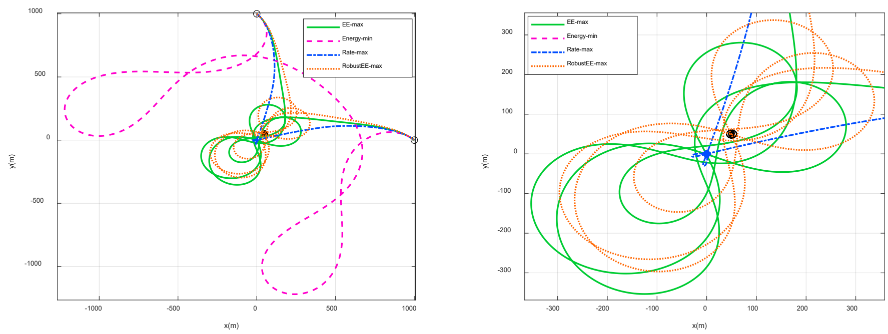

(a) The overall trajectory of the UAV (b) The local trajectory of the UAV

Fig. 3. The comparison of the UAV trajectory under different optimization schemes

The comparison of the projection results of the UAV trajectory in the horizontal plane between the proposed scheme and the other three schemes is illustrated in Fig. 3. The three schemes based on deterministic models are all proposed by [16]. The EE-max scheme represents an energy efficiency optimization based on the deterministic model, while the Energy-min scheme focuses on minimizing UAV propulsion energy consumption, and the Rate-max scheme aims to maximize communication rate. The user location information is known in the EE-max, Energy-min, and Rate-max schemes, where the user location is fixed at [0, 0]. In the RobustEE-max scheme, uncertainties arising from environmental interference and other factors are taken into account when acquiring the user location in emergency rescue environments. Therefore, the user location is described by an estimated coordinate of $\tilde{\mathbf{p}} = [50, 50]^T$ with an estimation error of $\varepsilon = 10$. The flight time is $T = 260s$. The overall results of the UAV trajectory optimization for the four schemes are depicted in Fig. 3(a), while Fig. 3(b) illustrates the local results of the UAV trajectory optimization.

The UAV trajectory optimized by the Energy-min scheme, as shown in Fig. 3(a), exhibits a large turning radius and predominantly flies in a straight line. This is because the scheme aims to minimize propulsion energy consumption, leading to reduced energy usage during turns. Additionally, under the scheme, the UAV remains distant from the ground user location due to its sole focus on minimizing propulsion energy consumption without considering communication requirements between the UAV and the ground user. Consequently, it can be concluded that the Energy-min scheme fails to strike a balance between energy consumption and communication quality. As shown in Fig. 3(b), it can be observed that the UAV, operating under the Rate-max scheme, follows a direct trajectory from its initial position to directly above the user location in the sky. Subsequently, it hovers over the user with a minimal turning radius and then continues on a straight path towards the final position. This is because the scheme aims to maximize the communication rate between the UAV and the ground user, disregarding energy consumption resulting from UAV turning maneuvers. Consequently, while hovering around the user, the UAV maintains a very small turning radius. Although communication requirements are considered in the scheme, it overlooks energy consumption associated with a reduced turning radius. It demonstrates that the Rate-max scheme still fails to address both the issues of energy consumption and communication quality. The optimized trajectory of the EE-max scheme is illustrated in Fig. 3(b). In this approach, the UAV follows a path resembling the shape of an "8" and strategically hovers over the user with an appropriate turning radius to ensure a sufficient communication distance while meeting all communication requirements. Hence, the scheme outperforms both the Energy-min scheme and Rate-max scheme. However, these three schemes optimize the UAV trajectory based on a deterministic model without accounting for uncertainty in the user position. In emergency rescue scenarios where complete knowledge of user location is absent, these optimization schemes become impractical. The UAV in the figure, following the RobustEE-max scheme, also adopts an "8" shaped trajectory while flying over the user. There is a difference in terms of the user's position when compared to the other three schemes. The discrepancy arises from incorporating the positional uncertainty of the ground user into the model, which is represented by utilizing the estimated coordinate and estimation error. The optimization results of the proposed scheme and three other schemes demonstrate its effectiveness in balancing energy consumption and communication throughput while accommodating uncertainties caused by environmental interference at the user's position. Thus, validating the effectiveness of the proposed scheme even under scenarios involving deviations in the user's position.

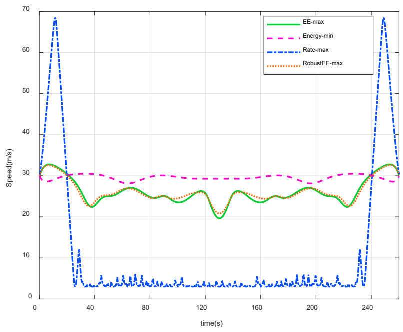

Fig. 4. The comparison of UAV speed under different optimization schemes

The variation in UAV flight speed for the four schemes corresponding to Fig. 3 is illustrated in Fig. 4. In the Energy-min scheme, the speed is maintained at the energy-minimum value [16] $V_{em} = 30\mathrm{m} / \mathrm{s}$. The purpose of this selection is to optimize the propulsion energy consumption by maintaining the speed value, in order to ensure a large turning radius and ultimately achieve the goal of minimizing the propulsion energy consumption. In the Rate-max scheme, the UAV initially reaches a higher speed level in less time, but then immediately slows down. It maintains a minimum speed value of approximately 3m/s for 200s and finally returns to a higher speed level again, corresponding to the flight trajectory shown in Fig. 3. The reason behind this is that the Rate-max scheme aims to optimize communication rate. However, the scheme does not take into account that too small of a turning radius will result in excessive energy consumption for the UAV. In the EE-max scheme, the speed is maintained in close proximity to the energy-minimum value $V_{em} = 30\mathrm{m} / \mathrm{s}$. The scheme aims to optimize energy efficiency, meet communication requirements without excessive propulsion energy consumption, and achieve the objective of energy-efficient communication. The speed in the RobustEE-max scheme is maintained close to the energy-minimum value $V_{em} = 30\mathrm{m} / \mathrm{s}$, as maximizing robust energy efficiency is a primary objective of the scheme. Despite incorporating the uncertainty of the user coordinate into the model, the proposed scheme effectively fulfills both energy consumption and communication quality requirements for the UAV. Comparing variations in UAV speed across all four schemes demonstrates the effectiveness of the proposed scheme in adapting to uncertainty in user position information.

The comparison of the average communication rate between the proposed scheme and the other three schemes is shown in Fig. 5. The Energy-min scheme is represented by "□", the Rate-max scheme is represented by "○", the EE-max scheme is represented by "Δ", and the RobustEE-max scheme is represented by "◊". In the four optimization schemes, the selection of ground user position coordinates remains unchanged as mentioned above. The UAV flight time is $T = 200s$. The figure shows that, the average communication rate of the Rate-max scheme remains at its highest level. The reason for this is that it does not take into account energy consumption for propulsion. In order to maximize the air-ground communication rate, it hovers over the user with a small turning radius for an extended period of time to maintain the closest communication distance with the user, which ensures high-quality communication between the UAV and the ground user. Therefore, the average communication rate curve of the scheme is consistently higher. On contrary to this scheme, the Energy-min scheme aims to optimize energy consumption without considering communication rate. As a result, the overall trajectory selects a path with large turning radius to minimize thrust energy consumption but sacrifices on communication rate. Hence, the Energy-min scheme has worst overall communication rates. The EE-max scheme aims to maximize communication energy efficiency, ensuring a balance between energy consumption and communication rate. Therefore, the average communication rate of the EE-max scheme is maintained at an intermediate level. Finally, the RobustEE-max scheme successfully achieves the objective of maximizing robust energy efficiency in emergency rescue scenarios by simultaneously considering communication rate and UAV energy consumption. Consequently, the average communication rate of this scheme is effectively maintained at a moderate level.

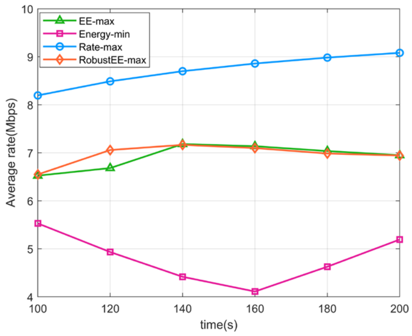

Fig. 5. The comparison of average communication rate under different optimization schemes

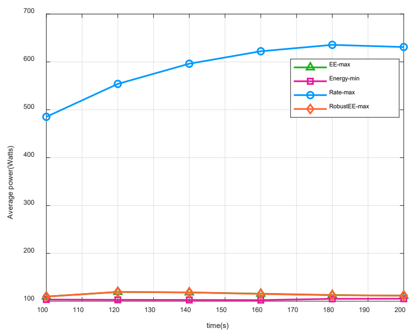

Fig. 6. The comparison of average power under different optimization schemes

The variation in UAV propulsion energy consumption for the proposed scheme and three different schemes is illustrated in Fig. 6. The Rate-max scheme solely focuses on communication rate, neglecting propulsion energy consumption. Consequently, the scheme exhibits a small turning radius in its flight trajectory, sacrificing thrust energy to enhance communication throughput, which explains its highest energy consumption as depicted in Fig. 6. The Energy-min scheme aims to minimize energy consumption and mostly relies on large turning radius in its trajectory, resulting in longer communication distances with the user and lower communication rates but keeping its energy consumption at the lowest level. The EE-max scheme balances UAV energy efficiency and communication rate by considering factors of UAV flight energy consumption. Therefore, the energy consumption curve of the scheme remains low in figure. Finally, the RobustEE-max scheme, which aims to achieve robust energy efficiency, also takes into account the propulsion energy consumption, thereby maintaining a low level of energy consumption in the figure.

Fig. 7 illustrates the variation in the energy efficiency between the proposed scheme and three other different schemes. The Rate-max scheme solely optimizes communication rate without considering energy consumption, resulting in the UAV sacrificing thrust energy to increase communication throughput while flying. Consequently, it exhibits the worst energy efficiency among all schemes. The Energy-min scheme selects paths with larger turning radius to minimize thrust energy consumption, however this means sacrificing throughput. Thus, it is also shown as a poor level. The EE-max scheme aims to optimize energy efficiency and is represented at a high level. On the other hand, the RobustEE-max scheme optimizes trajectory by considering uncertainties regarding ground user position for robust energy efficiency. By hovering over the user using an "8" trajectory, the scheme achieves higher communication throughput while ensuring minimum propulsion energy consumption, thus achieving optimal total energy efficiency. Comparing the results of different optimization schemes reveals that the proposed scheme can overcome inaccuracies in acquiring user location information and meet requirements for efficient UAV airborne communication, highlighting its effectiveness and robustness.

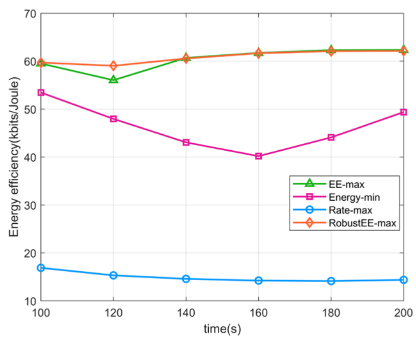

Fig. 7. The comparison of the energy efficiency under different optimization schemes

Fig. 8 illustrates the impact of changes in ε on the UAV trajectory optimization. In the proposed scheme, the model incorporates the estimated coordinate and estimation error to account for uncertainty. Therefore, to demonstrate the impact of changes in ε on the UAV trajectory, assuming that the estimated coordinate is $\tilde{\mathbf{p}} = [50, 50]^T$, and the estimated error is $\varepsilon = \{10, 40, 100\}$. Fig. 8(a) illustrates the global and local UAV trajectories for $T = 100s$. Fig. 8(b) illustrates the global and local UAV trajectories for $T = 150s$. Fig. 8(c) shows the global and local UAV trajectories for $T = 200s$. Fig. 8(d) shows the global and local UAV trajectories for $T = 250s$. As a whole, as ε increases, the turning radius of the UAV hovering over the user also increases. This is because the estimation error grows, resulting in increasingly inaccurate location information of the user. To overcome the uncertainty caused by an increase in ε on the model's performance, it is necessary for the UAV to fly with a larger turning radius to ensure a broader coverage area and achieve effective communication with the user. This demonstrates that the proposed scheme can mitigate uncertainty related to the user location information and ultimately improve communication quality and energy efficiency by optimizing UAV trajectory.

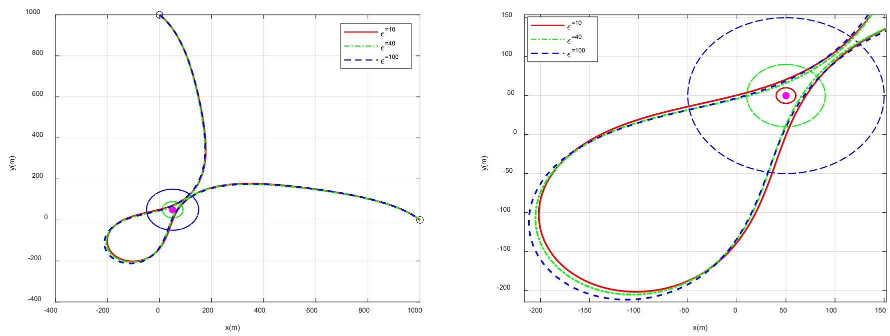

(a) $T = 100s$, $\varepsilon = \{10, 40, 100\}$ UAV trajectory

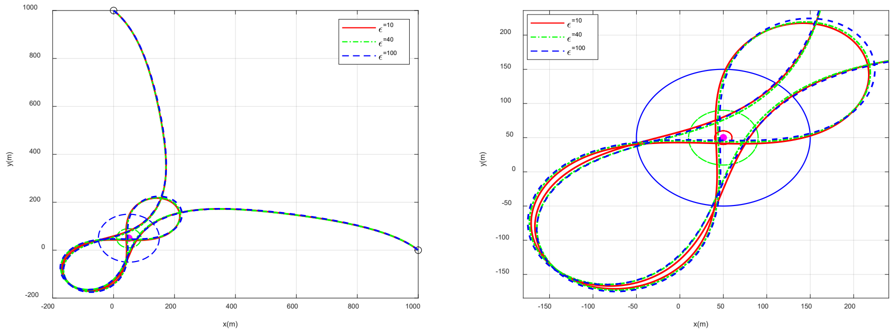

(b) $T = 150s$, $\varepsilon = \{10, 40, 100\}$ UAV trajectory

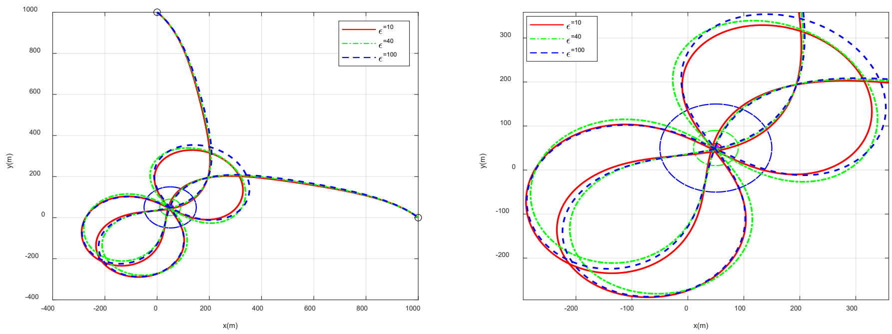

(c) $T = 200s$, $\varepsilon = \{10, 40, 100\}$ UAV trajectory

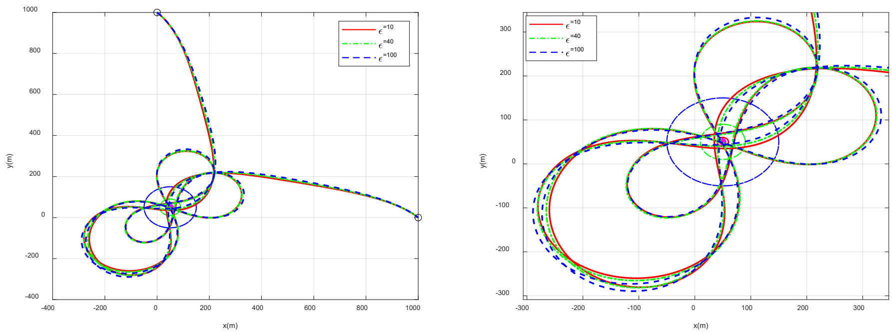

(d) $T = 250s$, $\varepsilon = \{10, 40, 100\}$ UAV trajectory

Fig. 8. The impact of ε on the UAV trajectory

Fig. 9 illustrates the effect of changes in ε on the UAV speed, corresponding to the trajectory optimization results shown in Fig. 8. Similarly, assuming that the estimated coordinate is $\tilde{\mathbf{p}} = [50, 50]^T$, and the estimated error is $\varepsilon = \{10, 40, 100\}$. Fig. 9(a) shows the variations in speed for $T = 100s$, Fig. 9(b) shows the variations in speed for $T = 150s$, Fig. 9(c) displays the variations in speed for $T = 200s$, and Fig. 9(d) presents the variations in speed for $T = 250s$. In Fig. 9(a), the speed increases as ε increases during flight times ranging from 30s to 70s. In Fig. 9(b), a similar increase in speed is observed during flight times ranging from 30s to 40s, from 55s to 65s, from 85s to 95s, and from 110s to 120s. In Fig. 9(c), an increase in speed is observed during flight times ranging from 30s to 50s, from 70s to 130s, and from 150s to 170s. In Fig. 9(d), an increase in speed is observed during flight times ranging from 30s to 90s, from 100s to 110s, from 130s to 140s, and from 150s to 210s. On the whole, as ε increases, the speed increases. The reason for this is that, in order to overcome uncertainty regarding the user location information at the same time, the UAV adopts a trajectory with a larger turning radius and increased flight distance, resulting in an increased speed. Additionally, as time progresses, there are different periods where the speed increases due to optimized trajectories varying. However, these concentrated periods of speed increase occur when the UAV hovers over the user. This demonstrates that the proposed scheme can adapt to uncertainty introduced by the user location information within the model and achieve energy-efficient communication objectives.

The impact of changes in ε on the energy efficiency is illustrated in Fig. 10. The dotted line with $\varepsilon = 0$ represents the change in the energy efficiency optimized by the scheme proposed in [16], which does not consider the uncertainty of the user location. $\varepsilon = \{10, 20, 40, 60, 80, 100\}$ represents changes in energy efficiency optimized by the proposed scheme. Overall, as ε increases, the energy efficiency decreases. The rationale behind this paper lies in its focus on the emergency communication scenario with inherent uncertainty, and the proposed scheme serves as a means to ensure that the UAV emergency communication model remains unaffected by worst-case uncertainty. In other words, it exhibits a certain degree of conservatism which ultimately contributes to its robustness. In addition, with the decrease of time, both the EE-max scheme and the proposed scheme exhibit a decreasing trend in the energy efficiency. The energy efficiency of the EE-max scheme is reduced by 4.54%. When $\varepsilon = 10$, the robust energy efficiency of the proposed scheme decreases by 3.90%, and its robustness is 0.64% better than that of the EE-max scheme. When $\varepsilon = 20$, the energy efficiency is reduced by 3.91%, and the robustness is improved by 0.63%. When $\varepsilon = 40$, the energy efficiency is reduced by 3.87%, and the robustness is improved by 0.67%. When $\varepsilon = 60$, the energy efficiency is reduced by 3.82%, and the robustness is improved by 0.72%. When $\varepsilon = 80$, the energy efficiency is reduced by 3.76%, and the robustness is improved by 0.78%. When $\varepsilon = 100$, the energy efficiency is reduced by 3.67%, and the robustness is improved by 0.87%.

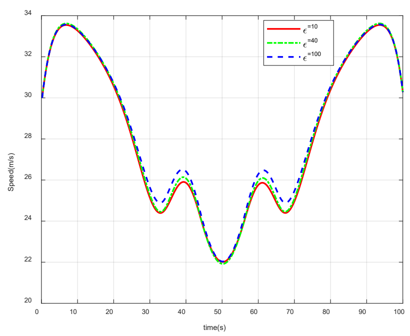

(a) $T = 100s$, $\varepsilon = \{10, 40, 100\}$

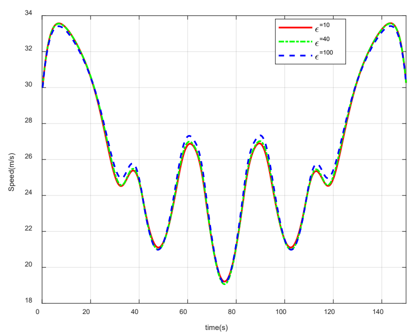

(b) $T = 150s$, $\varepsilon = \{10, 40, 100\}$

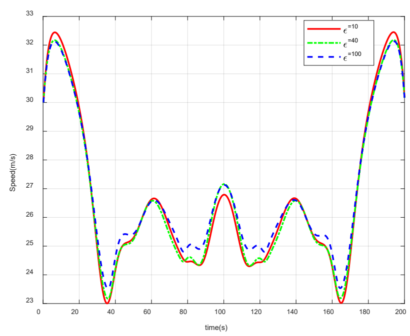

(c) $T = 200s$, $\varepsilon = \{10, 40, 100\}$

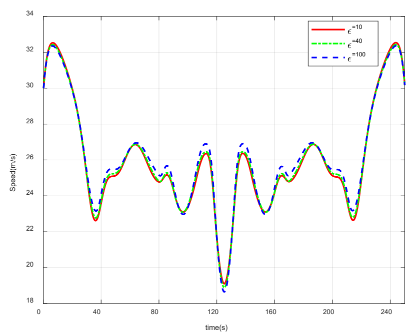

(d) $T = 250s$, $\varepsilon = \{10, 40, 100\}$

Fig. 9. The impact of changes in ε on the UAV speed

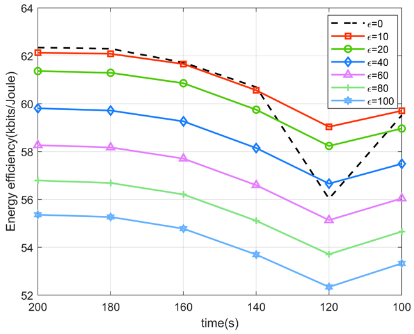

Fig. 10. The impact of changes in ε on the energy efficiency

The above analysis shows that as ε gradually increases, the decrease ratio of the robust energy efficiency optimized by the proposed scheme slows down gradually. The optimized scheme exhibits a 0.87% higher level of robustness compared to the EE-max scheme when $\varepsilon = 100$, thereby demonstrating the commendable robustness of the proposed approach. The reason for this is that as ε grows and accumulates, it becomes infeasible for the deterministic optimization model-based EE-max scheme to function effectively. On the other hand, the proposed scheme aims to ensure that even in the worst-case scenario of uncertainty, optimal robust energy efficiency remain within a stable range. This further demonstrates the proposed scheme successfully mitigates uncertainties caused by inaccurate user location information and effectively improves overall system robustness.

The impact of changes in ε on the average communication rate is shown in Fig. 11. The dotted line with $\varepsilon = 0$ represents the change in the average communication rate optimized by the scheme proposed in [16]. $\varepsilon = \{10, 20, 40, 60, 80, 100\}$ represents the changes of the average communication rate optimized by the proposed scheme. As ε increases, the average communication rate decreases. This is because the focus of this paper is to consider the uncertainty in acquiring the user location and ensure stable communication quality in the emergency communication scenario. That's the conservative explanation above. Moreover, as time decreases, the optimized average communication rate of both the EE-max scheme and the proposed scheme show a decreasing trend. The average communication rate of the EE-max scheme ($\varepsilon = 0$) decreases by 6.12%. When $\varepsilon = 10$, the average communication rate of the proposed scheme decreases by 5.66%, and the robustness is 0.46% higher than that of the EE-max scheme. When $\varepsilon = 20$, the average communication rate is reduced by 5.73%, and the robustness is improved by 0.39%. When $\varepsilon = 40$, the average communication rate is reduced by 5.67%, and the robustness is improved by 0.45%. When $\varepsilon = 60$, the average communication rate is reduced by 5.65%%, and the robustness is improved by 0.47%. When $\varepsilon = 80$, the average communication rate is reduced by 5.39%, and the robustness is improved by 0.73%. When $\varepsilon = 100$, the average communication rate is reduced by 5.19%, and the robustness is enhanced by 0.93%.

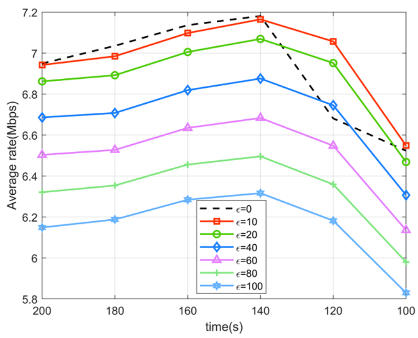

Fig. 11. The impact of changes in ε on the average rate

The above analysis shows that as ε gradually increases, the reduction rate of the average communication rate optimized by the proposed scheme decreases gradually. the robustness of the proposed scheme is improved by 0.93%, when $\varepsilon = 100$. The proposed scheme overcomes the uncertainty caused by inaccurate location information of the ground user, as demonstrated by analyzing the impact of changes in ε on the average communication rate.

The performance values of the proposed optimization scheme are given in Table 4, along with the mean and standard deviation for each performance metric. In the experiment, the estimated coordinate is $\tilde{\mathbf{p}} = [50,50]^T$, the estimation error is $\varepsilon = 10$, the running time is $T = 100s$. The experiment is repeated 10 times. The deviations of the values for energy efficiency, average communication rate, energy consumption, speed, and acceleration across 10 times do not exceed ±0.01%, indicating the effectiveness and robustness of the proposed scheme. The comparison of the values at 5 and 8 times reveals that, a lower energy consumption value corresponds to a higher energy efficiency value at an equal communication rate. Comparing the values at 9 and 10 times shows that, for an equal energy consumption value, a higher average communication rate leads to a higher energy efficiency value. This suggests that achieving a balance between communication quality and energy consumption is necessary.

Table 4. The performance values

No.	Energy efficiency (kbits/Joule)	Average communication rate (Mbps)	Average power (Watts)	Average speed (m/s)	Average acceleration (m/s^2)
1	59.705	6.549	109.684	28.310	2.209
2	59.705	6.549	109.684	28.310	2.209
3	59.707	6.549	109.684	28.309	2.210
4	59.703	6.549	109.685	28.310	2.209
5	59.708	6.549	109.684	28.309	2.210
6	59.701	6.548	109.685	28.310	2.209
7	59.700	6.548	109.686	28.310	2.209
8	59.710	6.549	109.683	28.309	2.210
9	59.702	6.548	109.684	28.310	2.210
10	59.708	6.549	109.684	28.310	2.209
Mean	59.7049	6.5487	109.6843	28.3097	2.2094
Std	0.0032	0.0004	0.0008	0.0005	0.0032

The performance values of the three different combinations are being compared in Table 5. The table provides values for energy efficiency, average communication rate, energy consumption, speed, and acceleration for each combination. Additionally, the mean and standard deviation of each performance metric are provided. The combination 1 corresponds to $\tilde{\mathbf{p}} = [0,0]^T$, with $\varepsilon = 10$. The combination 2 corresponds to $\tilde{\mathbf{p}} = [50,50]^T$, with $\varepsilon = 15$. The combination 3 corresponds to $\tilde{\mathbf{p}} = [100,100]^T$, with $\varepsilon = 20$. The experiment is repeated 5 times for each combination, and the running time is $T = 100s$. Table 5 shows that from combination 1 to 3, although ε is constantly increasing, both the energy efficiency values and the average communication rate values are also increasing. This is because the selection of estimated coordinates differs among the three combinations. When the estimated coordinates selected are close to the midpoint between the starting point and end point of the UAV, they can partially offset the influence of the estimation error on performance. This demonstrates that in the proposed scheme, appropriate selection of the estimation coordinate and the estimation error can achieve the objective of energy-efficient communication in the presence of uncertainty.

The optimization of the UAV trajectory in an emergency rescue scenario is illustrated in Fig. 12. Sudden disasters cause most communication base stations to cease operations, resulting in interrupted communication in the severely affected area [29]. Based on the emergency relief scenario, and considering the inaccuracy of acquiring the information of the position in the affected area due to disaster interference, the flight trajectory of the fixed-wing UAV is simulated in order to maximize robust energy efficiency. Assuming a length ratio of 1:100000, the estimated coordinate of the user in the disaster area is $\tilde{\mathbf{p}} = [-200,0]^T$, the estimated error is $\varepsilon = 20$, and the running time is $T = 250s$. It can be observed that the UAV hovers in the shape of an "8" over the disaster area to provide the emergency communication service, indicating that the proposed scheme adapts to uncertainty caused by inaccurate location information and optimizes the trajectory of the UAV. The proposed scheme is proven to effectively solve practical problems and possesses valuable applications.

Table 5. The performance values of the three different combinations

Combination	No.	Energy efficiency (kbits/Joule)	Average communication rate (Mbps)	Average power (Watts)	Average speed (m/s)	Average acceleration (m/s^2)
Combination 1 $\tilde{\mathbf{p}} = [0,0]^T$ $\varepsilon = 10$	1	58.777	6.446	109.672	28.534	2.162
	2	58.779	6.446	109.672	28.533	2.162
	3	58.775	6.446	109.673	28.534	2.162
	4	58.773	6.446	109.673	28.535	2.162
	5	58.781	6.447	109.672	28.533	2.163
	Mean	58.777	6.4462	109.6724	28.5338	2.1622
	Std	0.0028	0.0004	0.00049	0.0007	0.0004
Combination 2 $\tilde{\mathbf{p}} = [50,50]^T$ $\varepsilon = 15$	1	59.333	6.509	109.699	28.328	2.213
	2	59.334	6.509	109.699	28.328	2.213
	3	59.332	6.509	109.700	28.328	2.213
	4	59.335	6.509	109.699	28.328	2.213
	5	59.338	6.509	109.698	28.327	2.213
	Mean	59.3344	6.509	109.699	28.3278	2.213
	Std	0.0021	0.0002	0.0006	0.0004	0.0001
Combination 3 $\tilde{\mathbf{p}} = [100,100]^T$ $\varepsilon = 20$	1	59.756	6.554	109.687	28.252	2.267
	2	59.760	6.555	109.682	28.256	2.267
	3	59.754	6.554	109.690	28.249	2.267
	4	59.755	6.554	109.688	28.250	2.266
	5	59.759	6.555	109.683	28.254	2.267
	Mean	59.7568	6.5544	109.686	28.2522	2.2666
	Std	0.0023	0.0005	0.0030	0.0026	0.0005

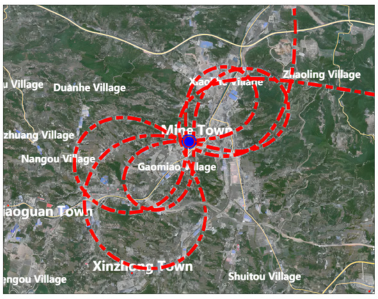

Fig. 12. The trajectory of the UAV in an emergency rescue scenario

6 Conclusion

In response to the challenge of incomplete information regarding the location of a user and limited energy resources in UAV-assisted emergency communication, a robust energy efficiency optimization strategy in emergency communication is proposed in this paper based on fixed-wing UAVs. The simulation experiments are designed to verify the worst-case robustness of the proposed approach and discuss the impact of the estimation error on the model. The simulation results demonstrate that the proposed strategy can achieve trajectory optimization of UAVs in the presence of an uncertain user position and enable energy-efficient communication. Furthermore, compared to the schemes of maximizing rate and minimizing energy consumption, the proposed strategy significantly enhances the value of energy efficiency while also demonstrating superior robustness when compared to the deterministic method for optimizing energy efficiency. The focus of this paper is on the impact of uncertainty in the location on the emergency communication model. However, in actual scenarios, widespread uncertainties that may lead to changes in the model structure when multiple uncertainties coexist occur. Therefore, further research is needed to optimize the emergency communication model in such circumstances.

7 Acknowledgement

This work was supported by National Natural Science Foundation of China (Grant No. 61802107), and Science and Technology Research Project of Higher Education Institutions of Hebei Province (Grant No. ZD2020171).

References

[1] J.X. Yang, Y.D. Fang, L. Bian, X.H. Huang, S.L. Liu, Z.Y. Jia, Research and application exploration of digital battlefield system for emergency rescue, China Safety Science Journal 33(10)(2023) 1-7.
[2] C.H. Zhong, J.P. Yao, J. Xu, Secure UAV communication with cooperative jamming and trajectory control, IEEE Communications Letters 23(2)(2019) 286-289.
[3] J.C. Gu, H.C. Wang, G.R. Ding, Y.T. Xu, Z. Xue, H.J. Zhou, Energy-constrained completion time minimization in UAV-enabled internet of things, IEEE Internet of Things Journal 7(6)(2020) 5491-5503.
[4] W. Wang, R.Q. Gu, H.Z. Liu, Y.Q. Hao, Robust optimization of UAV assisted internet of things based on parameter interval uncertainty analysis, Application Research of Computers 39(12)(2022) 3743-3749.
[5] M. Sinay, N. Agmon, O. Maksimov, G. Levy, M. Bitan, S. Kraus, UAV/UGV search and capture of goal-oriented uncertain targets, in: Proc. 2018 International Conference on Intelligent Robots and Systems, 2018.
[6] Y.B. Li, H.J. Zhang, K.P. Long, A. Nallanathan, Exploring sum rate maximization in UAV-based multi-IRS networks: IRS association, UAV altitude, and phase shift design, IEEE Transactions on Communications 70(11)(2022) 7764-7774.
[7] C. Zhan, Y. Zeng, Energy minimization for cellular-connected UAV: from optimization to deep reinforcement learning, IEEE Transactions on Wireless Communications 21(7)(2022) 5541-5555.
[8] J.X. Feng, S.S. Luan, J.M. Liu, C.S. Pan, An unmanned aerial vehicle trajectory planning method with high throughput, Computer Engineering 47(1)(2021) 172-181.
[9] G.C. Zhang, X.Q. Ou, M. Cui, Q.Q. Wu, S.D. Ma, W. Chen, Cooperative UAV enabled relaying systems: joint trajectory and transmit power optimization, IEEE Transactions on Green Communications and Networking 6(1)(2022) 543-557.
[10] F.Y. Cui, Y.L. Cai, M.J. Zhao, Joint trajectory design and power allocation for NOMA-based mobile-UAV communication networks, Journal of Hangzhou Dianzi University (Natural Sciences) 40(1)(2020) 14-20.
[11] X. Liu, Y.W. Liu, Y. Chen, L. Hanzo, Trajectory design and power control for multi-UAV assisted wireless networks: a machine learning approach, IEEE Transactions on Vehicular Technology 68(8)(2019) 7957-7969.
[12] X.W. Pang, N. Zhao, J. Tang, C. Wu, D. Niyato, K.-K. Wong, IRS-assisted secure UAV transmission via joint trajectory and beamforming design, IEEE Transactions on Communications 70(2)(2022) 1140-1152.
[13] Y. Zeng, J. Xu, R. Zhang, Energy minimization for wireless communication with rotary-wing UAV, IEEE Transactions on Wireless Communications 18(4)(2019) 2329-2345.
[14] K. Xiong, Y. Liu, L.T. Zhang, B. Gao, J. Cao, P.Y. Fan, K.B. Letaief, Joint optimization of trajectory, task offloading, and CPU control in UAV-assisted wireless powered fog computing networks, IEEE Transactions on Green Communications and Networking 6(3)(2022) 1833-1845.
[15] Z.J. Wang, R.K. Liu, Q.R. Liu, J.S. Thompson, M. Kadoch, Energy-efficient data collection and device positioning in UAV-assisted IoT, IEEE Internet of Things Journal 7(2)(2020) 1122-1139.
[16] Y. Zeng, R. Zhang, Energy-efficient UAV communication with trajectory optimization, IEEE Transactions on Wireless Communications 16(6)(2017) 3747-3760.
[17] S.B. Eom, H.O. Lee, J.H. Park, I.K. Lee, UAV-aided wireless communication designs with propulsion energy limitations, IEEE Transactions on Vehicular Technology 69(1)(2020) 651-662.
[18] B. Duo, Q.Q. Wu, X.J. Yuan, R. Zhang, Energy efficiency maximization for full-duplex UAV secrecy communication, IEEE Transactions on Vehicular Technology 69(4)(2020) 4590-4595.
[19] S.X. Li, B. Duo, M.D. Renzo, M.X. Tao, X.J. Yuan, Robust secure UAV communications with the aid of reconfigurable intelligent surfaces, IEEE Transactions on Wireless Communications 20(10)(2021) 6402-6417.
[20] B.Y. Liu, Y.Y. Wan, F.H. Zhou, Q.H. Wu, R.Q.Y. Hu, Robust trajectory and beamforming design for cognitive MISO UAV networks, IEEE Wireless Communications Letters 10(2)(2021) 396-400.
[21] W. Wang, X.R. Li, R. Wang, K. Cumanan, W. Feng, Z.G. Ding, O.A. Dobre, Robust 3D-trajectory and time switching optimization for dual-UAV-enabled secure communications, IEEE Journal on Selected Areas in Communications 39(11) (2021) 3334-3347.
[22] R. Miranda-colorado, L.T. Aguilar, Robust PID control of quadrotors with power reduction analysis, ISA Transactions 98(2020) 47-62.
[23] C.X. Mu, Y. Zhang, Learning-based robust tracking control of quadrotor with time-varying and coupling uncertainties, IEEE Transactions on Neural Networks and Learning Systems 31(1)(2020) 259-273.
[24] W.L. Fan, Y. Wu, S.H. Ju, K. Zhang, W.W. Yang, Secure UAV communication with robust communication and trajectory design, in: Proc. 2019 International Conference on Computer, Information and Telecommunication Systems, 2019.

[25] Y.Y. Zhang, W. Ma, B. Li, Trajectory optimization for communication between energy-constrained UAV and moving ship, Chinese Journal of Ship Research 17(4)(2022) 47-56.
[26] A. Zappone, E. Jorswieck, Energy efficiency in wireless networks via fractional programming theory, Foundations and Trends in Communications and Information Theory 11(3-4)(2014) 185-396.
[27] F.Y. Yuan, B.Q. Xiao, K. Liu, Z.H. Dai, Analysis of taylor seriers method for TMA, Command Control and Simulation 44(1)(2022) 38-43.
[28] M. Grant, S. Boyd, CVX: Matlab software for disciplined convex programming, version 2.1. <http://cvxr.com/cvx> , 2014.
[29] F.C. Li, Y.S. Pei, J.J. Wang, L. Zhang, Y. Qiu, Thought on the integrated space terrestrial information network- a perspective from “July 20 heavy rainstorm in Zhengzhou” emergency rescue, Mobile Communications 45(5)(2021) 81-85.